Am J Physiol Renal Physiol 305: F71–F79, 2013.
First published May 1, 2013; doi:10.1152/ajprenal.00694.2012.

Impaired EphA4 signaling leads to congenital hydronephrosis, renal injury, and hypertension

Johan Sällström,[1,2] Christiane Peuckert,[3] Xiang Gao,[1,3] Erik Larsson,[4] Anders Nilsson,[5] Boye L. Jensen,[6] Maristela L. Onozato,[7] A. Erik G. Persson,[1] Klas Kullander,[3] and Mattias Carlström[1,2]

[1]*Deptartment of Medical Cell Biology, Uppsala University, Uppsala, Sweden;* [2]*Department of Physiology and Pharmacology, Karolinska Institutet, Solna, Sweden;* [3]*Department of Neuroscience, Developmental Genetics, Uppsala University, Uppsala, Sweden;* [4]*Department of Genetics and Pathology, Uppsala University, Uppsala, Sweden;* [5]*Department of Oncology, Radiology and Clinical Immunology, Uppsala University, Uppsala, Sweden;* [6]*Department of Cardiovascular and Renal Research, Institute of Molecular Medicine, University of Southern Denmark, Odense, Denmark; and* [7]*Department of Pathology, Massachusetts General Hospital, Boston, Massachusetts*

Submitted 17 December 2012; accepted in final form 22 April 2013

Sällström J, Peuckert C, Gao X, Larsson E, Nilsson A, Jensen BL, Onozato ML, Persson AE, Kullander K, Carlström M. Impaired EphA4 signaling leads to congenital hydronephrosis, renal injury, and hypertension. *Am J Physiol Renal Physiol* 305: F71–F79, 2013. First published May 1, 2013; doi:10.1152/ajprenal.00694.2012.—Experimental hydronephrosis induced by partial ureteral obstruction at 3 wk of age causes hypertension and renal impairment in adult rats and mice. Signaling by Ephrin receptors (Eph) and their ligands (ephrins) importantly regulates embryonic development. Genetically modified mice, where the cytoplasmic domain of the *EphA4* receptor has been substituted by enhanced green fluorescent protein (*EphA4*$^{gf/gf}$), develop spontaneous hydronephrosis and provide a model for further studies of the disorder. The present study aimed to determine if animals with congenital hydronephrosis develop hypertension and renal injuries, similar to that of experimental hydronephrosis. Ultrasound and Doppler techniques were used to visualize renal impairment in the adult mice. Telemetric blood pressure measurements were performed in *EphA4*$^{gf/gf}$ mice and littermate controls (*EphA4*$^{+/+}$) during normal (0.7% NaCl)- and high (4% NaCl)-sodium conditions. Renal excretion, renal plasma flow, and glomerular filtration were studied, and histology and morphology of the kidneys and ureters were performed. *EphA4*$^{gf/gf}$ mice developed variable degrees of hydronephrosis that correlated with their blood pressure level. In contrast to *EphA4*$^{+/+}$, the *EphA4*$^{gf/gf}$ mice displayed salt-sensitive hypertension, reduced urine concentrating ability, reduced renal plasma flow, and lower glomerular filtration rate. Kidneys from *EphA4*$^{gf/gf}$ mice showed increased renal injuries, as evidenced by fibrosis, inflammation, and glomerular and tubular changes. In conclusion, congenital hydronephrosis causes hypertension and renal damage, similar to that observed in experimentally induced hydronephrosis. This study further reinforces the supposed causal link between hydronephrosis and later development of hypertension in humans.

ephrin; gene modified mice; human disorder; receptor; ureteral obstruction

CONGENITAL ANOMALIES OF THE kidney and urinary tract include a wide range of renal and urinary tract malformations and are detected in ~0.2–2% of all newborns (35). One of the most prevalent urological anomalies that can lead to renal insufficiency is congenital obstructive nephropathy (12). Histopathologically, the obstruction frequently becomes manifest as hydronephrosis (19, 24). Several underlying mechanisms for obstructive nephropathy have been identified, such as developmental abnormalities of the urinary collecting system as seen in duplicate collecting systems, posterior urethral valves or parenchyme malformations as renal dysplasia, renal agenesis, renal tubular dysgenesis, and polycystic renal diseases (2). The familiar accumulation of congenital kidney and urinary tract anomalies indicates that a genetic component may be involved in its formation. (11, 16, 32).

Although congenital urinary tract obstruction is a common disorder in infants, its pathophysiology remains poorly understood and its clinical management has been debated among urologists for many years. Studies have demonstrated that kidney function, in terms of renal perfusion and glomerular filtration remains, rather well preserved during infancy in hydronephrosis (3, 15, 34). These observations have led to a worldwide trend towards nonoperative management in children with nonsymptomatic unilateral hydronephrosis, but the long-term physiological consequences of this new policy are unclear (4). We have previously demonstrated that experimentally induced hydronephrosis, after completed nephrogenesis, is associated with renal injuries and is causally related to hypertension in both rats (5, 9) and mice (6, 8). However, the potential link between congenital hydronephrosis and later development of hypertension and renal dysfunction has not been investigated.

Eph receptors constitute the largest known family of receptor tyrosine kinases and are involved in the modulation of the cytoskeleton and in regulation of cell adhesion and migration (17). During development, Eph receptors and their ligands (i.e., ephrins subclass A and B) have central functions in patterning the embryo in somitogenesis, in neuronal circuit formation, and in angiogenesis (10, 13, 17, 26–28). Genetically modified mice, where the cytoplasmic domain of the *EphA4* receptor has been substituted by enhanced green fluorescent protein (*EphA4*$^{gf/gf}$), develop spontaneous hydronephrosis due to the importance of intact Ephrin-Eph receptor signaling in embryonic development. Therefore, *EphA4*$^{gf/gf}$ mice are of interest for studying long-term consequences of congenital hydronephrosis on renal and cardiovascular function.

The aim of the present study was to further investigate the suggested link between congenital hydronephrosis and later development of hypertension and renal damage. Using *EphA4*$^{gf/gf}$ mice and littermate controls (*EphA4*$^{+/+}$), we hypothesized that animals with congenital hydronephrosis would develop hypertension, renal dysfunction, and kidney injuries similar to those observed in experimentally induced hydronephrosis.

Address for reprint requests and other correspondence: M. Carlström, Dept. of Physiology and Pharmacology, Karolinska Institutet, Nanna Svartz Väg 2, S-17177 Stockholm, Sweden (e-mail: mattias.carlstrom@ki.se).

MATERIALS AND METHODS

EphA4$^{gf/gf}$ mice, generated as earlier described (17), and their corresponding wild-type littermates (*EphA4$^{+/+}$*) were bred at the department and genotyped by PCR. The experiments were performed in 3- to 10-mo-old male and female mice from the breeding colony. Like in humans, hydronephrosis is occasionally found also in mice. In the present study, a small number of C57BL/6 mice with spontaneous hydronephrosis were included. These mice were discovered during routine induction of experimental hydronephrosis in 3-wk-old wild-type mice. In these mice, the abdomen was closed and blood pressure measurements were conducted at 3 mo of age. Corresponding sham-operated littermates (C57BL/6), with normal appearance of the kidneys, were used as control animals.

The animals were given a standardized normal-salt diet (0.7% NaCl, SD389-R36; Lactamin) followed by a high-salt diet (4% NaCl, SD312-R36; Lactamin, Kimstad, Sweden).

Ultrasound investigation of renal anomalies. Animals were anaesthetized with isoflurane (Forene; Abbot Scandinavia, Kista, Sweden), the fur above the position of the kidneys was shaved, and water-based ultrasound gel was applied. The kidneys were examined at 15 MHz with a linear high-frequency ultrasound transducer (Sequoia; Siemens-Acuson, Mountainview, CA). The built in Doppler feature was used to visualize blood flow in the kidney.

Telemetric measurements. A telemetric device (PA-C10; DSI, St. Paul, MN) was implanted in adult mice in the same way as earlier described (8). In short, isoflurane gas anesthesia was used and the catheter of the transmitter was placed into the left carotid artery with the telemetric blood pressure device placed subcutaneously in the right flank. All animals were allowed to recover for at least 10 days before any measurements were performed. The telemetric measurements were performed as previously described (8). Cardiovascular data, in mice given a normal-salt diet, were continuously collected for at least 48 h. After completion of the measurements, the diet was changed to a high-sodium diet and the animals were kept on this diet for 10 days whereupon cardiovascular data were collected for another 48 h.

Renal plasma flow and glomerular filtration. Renal plasma flow (RPF) was measured as the clearance of para-amino hippuric acid (PAH), and glomerular filtration rate (GFR) was measured by inulin clearance. These parameters were measured in conscious animals on a normal-sodium diet as previously described (30). In short, animals were given a bolus injection of [^{3}H]methoxy-inulin (ARC, St. Louis, MO) and of [^{14}C]PAH (PerkinElmer, Waltham, MA) dissolved in 200 μl saline into the tail vein whereupon blood samples were taken from the cut tip of the tail at 1, 3, 7, 10, 15, 35, 55, and 75 min. PAH and inulin clearances were calculated using noncompartmental pharmacokinetic data analysis as earlier described. RPF was estimated from the PAH clearance using a renal extraction ratio of 0.7. The filtration fraction (FF) was calculated from the ratio of RPF and GFR (FF = GFR/RPF).

Renal excretion measurements. The mice were placed in metabolism cages for 24 h, with food and water given ad libitum to study renal excretion of fluid and electrolytes. Water consumption and urine production were measured gravimetrically. Sodium and potassium concentrations were determined by flame photometry (FLM3; Radiometer, Copenhagen, Denmark) and urine osmolality by depression of the freezing point (Fiske 210 Micro-Sample Osmometer; Fiske Associates, Norwood, MA).

Renin measurements. Mice were anaesthetized as described above. Blood samples were taken from the carotid artery and immediately spun down using a cooled centrifuge, whereupon plasma was isolated and frozen in liquid nitrogen. PRC was measured by radioimmunoassay of angiotensin I, using the antibody-trapping technique described previously (22). Renin values were standardized by reference to renin standards (MRC; Holly Hill, London, UK) and expressed in Goldblatt units (GU).

Determination of hydronephrotic ratio. Once the renal and cardiovascular studies had been conducted, animals were anaesthetized as described above whereupon the abdomen was opened using a midline incision. A macroscopic examination of both kidneys was performed, and the hydronephrotic ratios (HNR) were calculated in the same way as earlier described (i.e., HNR = residual urine weight/renal parenchymal weight; Ref. 8). The kidneys were cut latitudinally and the middle part was used for histology.

Histology and morphology. Embryos at *day 15* (E15.5) and mice at postnatal *day 4* (P4) as well as kidneys from adult mice were fixed in formalin (4% in phosphate-buffered saline) for 12 h (embryos and pups) or 48 h (adult tissue) and embedded in paraffin. The tissue blocks were cut into 5-μm sections, stained with hematoxylin and eosin, periodic acid-Schiff, and picro-sirius, and a blinded histopathological evaluation was performed. Based on their HNRs, the kidneys of *EphA4$^{gf/gf}$* mice were grouped for the histopathological evaluation as the least or most affected kidney.

The renal cortex, medulla, and the papilla were investigated for fibrosis, inflammation (i.e., infiltration of mononuclear cells), tubular changes (i.e., atrophy, dilatation with hyaline cast deposition) and glomerular changes (i.e., sclerosis, epithelial cell proliferation, Bowman's space dilatation with periodic acid-Schiff-positive material deposition). The presence of glomerular change (G) was accessed and scored in 100 glomeruli in each section as G0 for a normal glomerulus; G1, mild sclerosis (<25%); G2, moderate segmental sclerosis (25–50%); and G3, severe segmental sclerosis (>50%). Tubular changes (T) were categorized semiquantitatively using a grading system as T0, normal; T1, focal tubular epithelial simplification with periarterial and peritubular fibrosis; and T2, multiple focal areas of tubular epithelial atrophy, dilatation with hyaline casts, and/or mononuclear cell infiltration in a large area. The damage score was calculated as (0 × number of S0 + 1 × number of S1 + 2 × number of S2 + 3 × number of S3)/(number of S0 + S1 + S2 + S3), where S represents glomerulosclerosis or tubulointerstitial injury.

Investigation of ureter morphology ex vivo. The bladder and the ureters from adult mice were dissected during immersion with PBS, and a ligature was placed around the ureters, close to the kidneys. Bromophenol blue solution (2 mg/ml in PBS) was injected into the bladder and allowed to perfuse at 4°C, and the morphology of the ureter lumen was studied and photographed.

Calculations and statistics. Values are presented as means ± SE. Statistics were calculated using GraphPad Prism 6 (GraphPad Software, La Jolla, CA). Single comparisons between normally distributed parameters were tested for significance with Student's paired or unpaired *t*-test. For multiple comparisons, two-way ANOVA (genotype and diet) followed by the Fisher's post hoc test was used. Scored data for the histological evaluation were analyzed by the Kruskal-Wallis test followed by the Mann-Whitney *U*-test. Statistical significance was defined as $P < 0.05$.

Ethics. The experiments were approved by the regional animal ethics committee in Uppsala and conducted in accordance with the National Institutes of Health *Guide for Care and Use of Laboratory Animals*.

RESULTS

At the time of the experiments there was no difference in body weight, age, or gender distribution between the *EphA4$^{gf/gf}$* and *EphA4$^{+/+}$* groups. *EphA4$^{gf/gf}$* mice displayed variable degrees of pelvic dilatation that was not seen in their littermate controls (Fig. 1). Bilateral hydronephrosis was evident in 17% of all investigated adult *EphA4$^{gf/gf}$* mice.

Ultrasound investigation of renal anomalies. The kidneys from *EphA4$^{gf/gf}$* mice displayed pelvic dilatation and reduced renal Doppler blood flow (Fig. 2).

Telemetric measurements. The hydronephrotic *EpA4$^{gf/gf}$* mice developed hypertension of different degrees. The blood pressure was significantly higher in the hydronephrotic animals than in the *EphA4$^{+/+}$* mice both during normal- and high-sodium conditions (Fig. 3). Furthermore, *EphA4$^{gf/gf}$* mice dis-

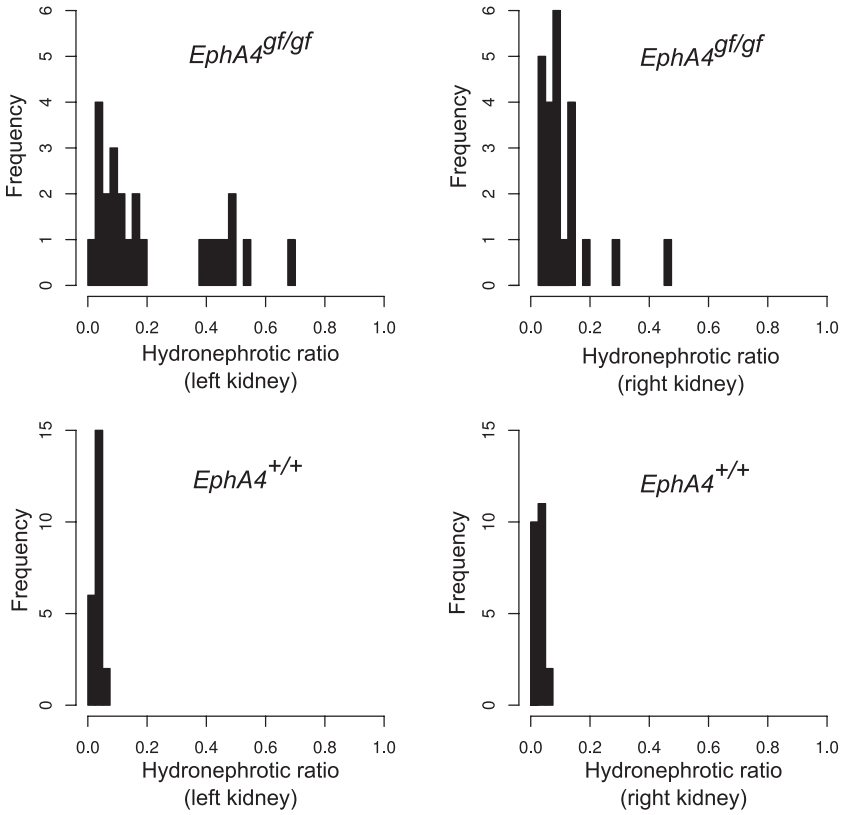

Fig. 1. Histogram of the hydronephrotic ratio (HNR) in the left and right kidney from all studied *EphA4*$^{gf/gf}$ and *EphA4*$^{+/+}$ control mice. Since most *EphaA4*$^{gf/gf}$ display unilateral rather than bilateral hydronephrosis, the histograms for the 2 genotypes overlap.

played salt-sensitive blood pressure, which was not found in the *EphA4*$^{+/+}$ group. The heart rate was not different between genotypes given the same diet. The high-salt diet did not significantly change heart rate in *EphA4*$^{gf/gf}$ ($P = 0.13$) or in *EphA4*$^{+/+}$ mice ($P = 0.09$). In *EphA4*$^{gf/gf}$ mice, the degree of hydronephrosis correlated with the blood pressure level and their salt sensitivity (i.e., increase in blood pressure in response to high-salt intake). No such correlation was observed in *EphA4*$^{+/+}$ mice (Fig. 4).

C57BL/6J mice ($n = 3$) with congenital hydronephrosis also displayed salt-sensitive hypertension (113 ± 1 to 122 ± 3 mmHg; HNR = 1.56 ± 0.49), which was not found in normal C57BL/6J ($n = 8$) controls (103 ± 3 to 105 ± 1; HNR = 0.04 ± 0.00).

Renal excretion, plasma flow, and glomerular filtration. The hydronephrotic mice had lower RPF and GFR compared with that of the *EphA4*$^{+/+}$ group (Fig. 5). No difference in FF was found between *EphA4*$^{gf/gf}$ (0.28 ± 0.02) and *EphA4*$^{+/+}$

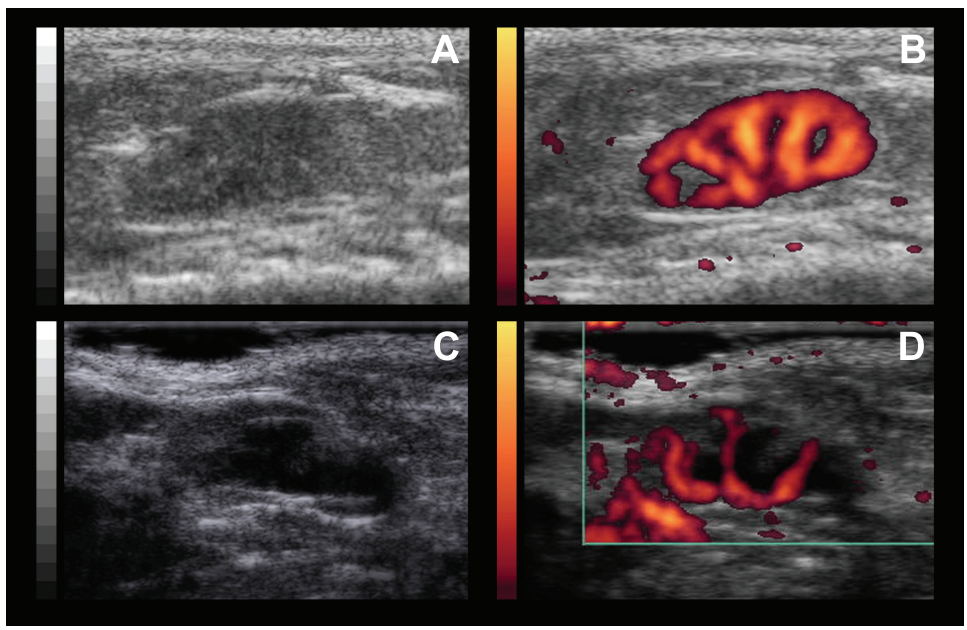

Fig. 2. Representative ultrasound and Doppler images of kidneys from *EphA4*$^{+/+}$ and *EphA4*$^{gf/gf}$ mice. Standard ultrasound image (*A* and *C*) shows kidney acoustic images. *EphA4*$^{gf/gf}$ kidney shows a large hypoechoic area representing the hydronephrotic pelvis with the parenchyma reduced to a narrow string to the periphery (*C*). *B* and *D*: Doppler ultrasound images of blood flow in yellow-red color in the same kidneys. Note the reduced blood flow in *D*. *A* and *B*: normal kidney from a control *EphA4*$^{+/+}$ mouse. *C* and *D*: kidney from a *EphA4*$^{gf/gf}$ mouse with hydronephrosis.

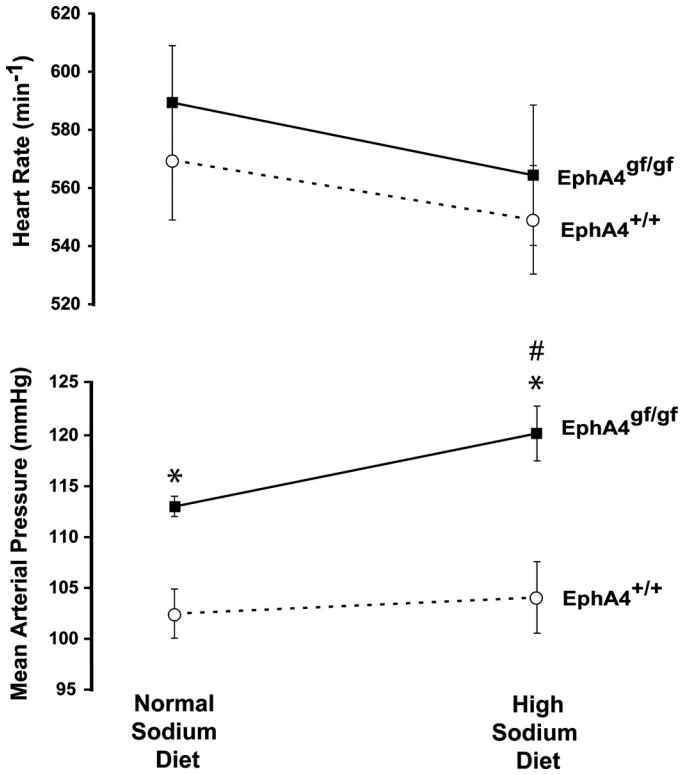

Fig. 3. Telemetric measurements in *EphA4*$^{gf/gf}$ ($n = 8$) and *EphA4*$^{+/+}$ ($n = 5$) mice during normal- and high-salt diet treatments. *EphA4*$^{gf/gf}$ mice with congenital hydronephrosis developed saltsensitive hypertension. Heart rate was not different between the genotypes. *$P < 0.05$, compared with *EphA4*$^{+/+}$ on same diet. #$P < 0.05$, compared with *EphA4*$^{gf/gf}$ on normal-sodium diet.

(0.27 ± 0.02) mice. Urine osmolality was reduced and urine production tended to be higher in *EphA4*$^{gf/gf}$ compared with the *EphA4*$^{+/+}$ mice (Fig. 5). HNR was significantly different in kidneys from *EphA4*$^{gf/gf}$ mice compared with *EphA4*$^{+/+}$ (0.38 ± 0.08 vs. 0.05 ± 0.01).

Plasma renin levels. There was no significant difference in PRC between *EphA4*$^{gf/gf}$ (2,481 ± 393; $n = 4$) and *EphA4*$^{+/+}$ (3,307 ± 710; $n = 5$) mice. HNR was significantly different in kidneys from *EphA4*$^{gf/gf}$ mice compared with *EphA4*$^{+/+}$ (0.20 ± 0.07 vs. 0.02 ± 0.01).

Histology and morphology. At the embryonic stage, *EphA4*$^{gf/gf}$ mice displayed duplex formations at different levels, bifid ureters, duplicated collecting system and duplex kidneys, but not hydronephrosis (Fig. 6). Postnatally those malformations were associated with hydronephrosis and hydroureter (observed penetrance 50%, $n = 35$; Fig. 7). The malformations were predominantly unilateral, but bilateral changes were also observed in 14% of the embryos and newborns.

The results from the renal histopathological evaluation of kidneys from adult mice are summarized in Table 1. Left and/or right kidneys of *EphA4*$^{gf/gf}$ mice displayed variable degrees of pelvic dilatation, with flattening of the renal medulla. The hydronephrotic kidneys exhibited areas with subepithelial fibrosis with infiltration of inflammatory mononuclear cells, tubular changes (i.e., atrophy, dilatation with hyaline cast deposition), and glomerular changes (i.e., sclerosis, mesangial matrix increase, and shrunken glomeruli). Glomerulosclerosis was the most predominant feature observed in this mice model with glomerular extracapillary proliferation, and cystic changes were rarely observed in this model. The histopathological changes in the least affected kidney were somewhat reduced compared with those of the most affected kidney. In *EphA4*$^{gf/gf}$ mice with unilateral hydronephrosis, increased histopathological changes were also found in the contralateral kidney. All *EphA4*$^{+/+}$ mice had normal HNR values (<0.05) and displayed normal histoarchitecture with no significant histopathological changes. Representative sections from *EphA4*$^{gf/gf}$ and *EphA4*$^{+/+}$ are shown in Fig. 8.

Ureter morphology. Injection of bromophenol blue into the bladder of the urogenital system dissected out from adult animals revealed morphological changes in ureters from hydronephrotic *EphA4*$^{gf/gf}$ mice (Fig. 7). The ureters were dilated and had a tortuous appearance compared with the straight shape of the controls, indicating impaired peristalsis.

DISCUSSION

In the present study, a genetic mouse model reveals a link between congenital hydronephrosis and later development of hypertension. Furthermore, the hydronephrotic animals used in this study displayed impaired renal function and kidney anomalies similar to that described in experimentally induced hydronephrosis (4).

Clinically, the incidence of postnatally confirmed urinary tract dilatation is reported to be 1–1.4% (21, 29, 33). The phenotype of the *EphA4*$^{gf/gf}$ mice is associated with a duplica-

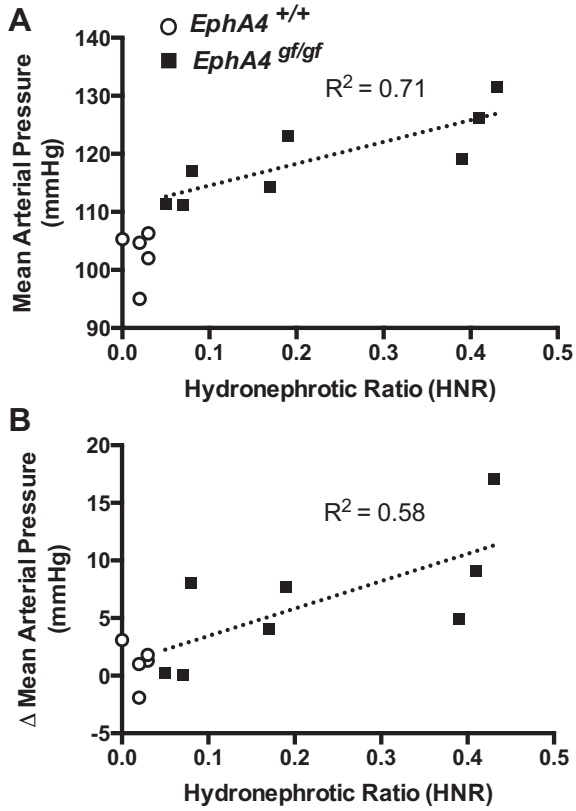

Fig. 4. Degree of hydronephrosis (HNR) correlated with the blood pressure level (*A*) and the salt sensitivity (*B*) in *EphA4*$^{gf/gf}$ mice ($n = 8$) but not in the control *EphA4*$^{+/+}$ mice ($n = 5$). Dashed line shows the linear regression within the *EphA4*$^{gf/gf}$ mice. In *EphA4*$^{+/+}$no correlation was found ($R^2 = 0.00$ in in *A* and *B*).

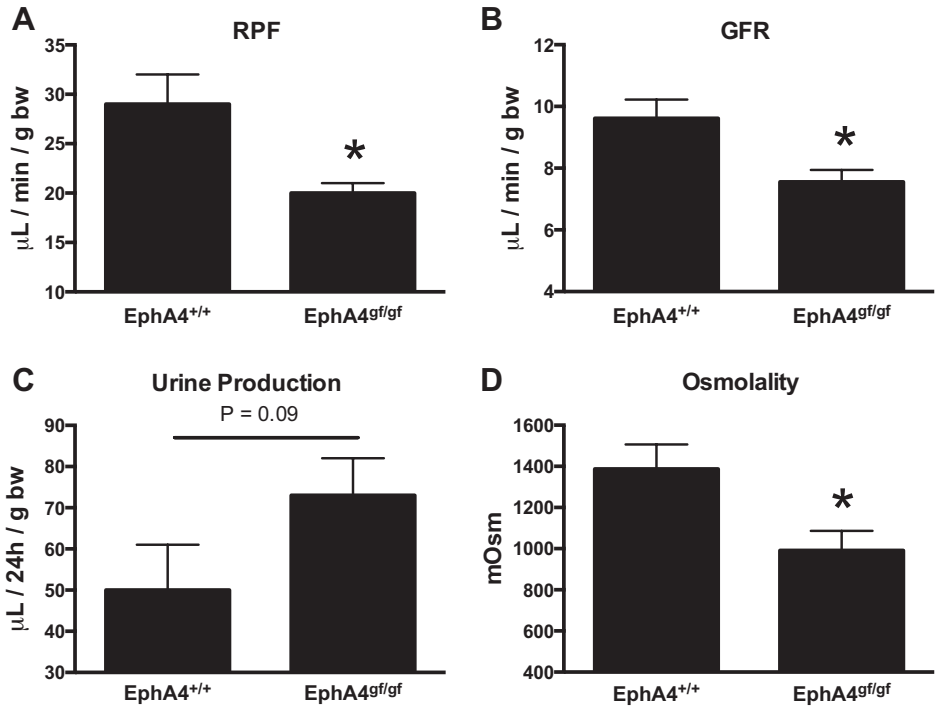

Fig. 5. Renal plasma flow (*A*), glomerular filtration rate (*B*), urine production rate (*C*), and osmolality (*D*) in *EphA4*$^{+/+}$ (n = 7) and *EphA4*$^{gf/gf}$ (n = 7–12; bw, body weight). *$P < 0.05$, compared with *EphA4*$^{+/+}$.

tion of the collecting system and the ureter. These changes are evident in the embryonic stage; however, hydronephrosis was only found in postnatal mice. In humans, duplications of the renal collecting system are considered to be common congenital anomalies and a combination of clinical reports and autopsies has yielded an incidence of 0.8% (31). In the clinic, duplex systems have been described to cause hydronephrotic changes as a consequence of ureteropelvic junction obstruction (1, 20, 25) and with an ectopic ureterocoele (24). Furthermore, hydronephrosis in *EphA4*$^{gf/gf}$ is associated with dilated and tortous ureters, which indicates impaired peristaltis. Consequently, the occurrence of hydronephrosis in *EphA4*$^{gf/gf}$ mice might be caused by ureteropelvic junction obstruction due to the observed duplex systems but could also be caused by impaired ureter peristaltis.

In humans, the hydronephrosis is usually found during routine prenatal ultrasound. Previously, surgical relief of the obstruction was routinely performed; however, during the last decade, nonoperative management has been applied if the patient displays normal renal function. At present, no systematic prospective study has been conducted to investigate the long-term consequences of the conservative treatment strategy in children with congenital hydronephrosis. However, there are several case reports on adult patients with hypertension that is obviously caused by hydronephrosis, as they became normotensive following nephrectomy or pyeloplasty (4). Recently, a

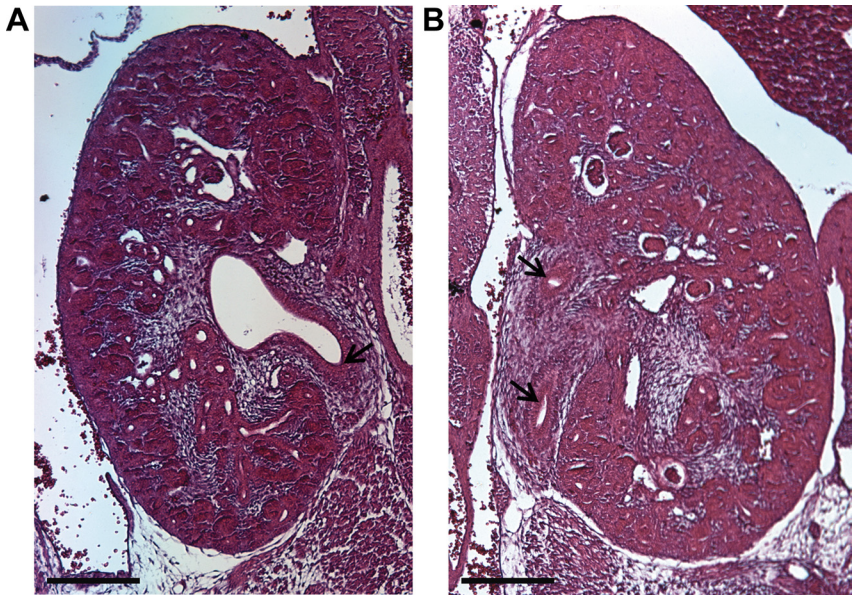

Fig. 6. Hematoxylin and Eosin-stained sections of kidneys from mouse embryos at embyonic *day 15.5*. *A*: kidney from a wild-type littermate with normal appearance. *B*: kidney from an *EphA4*$^{gf/gf}$ with duplicated ureters and with an incision at the upper pole indicating a partly duplex kidney. Arrows point out the ureters; scale bar = 250 µm.

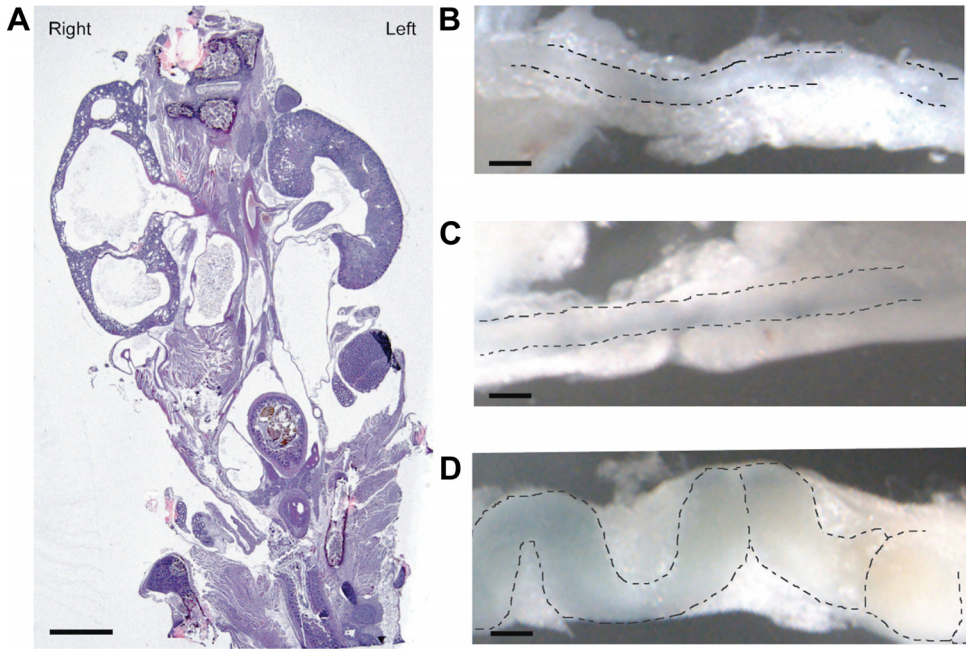

Fig. 7. *A*: hematoxylin and eosin-stained section of an *EphA4*$^{gf/gf}$ mouse at postnatal *day 4* with bilateral congenital hydronephrosis. Both kidneys display hydroureter. Right kidney displays a massively dilated collecting system whereas the dilatation is less pronounced in the left kidney. *B–D*: ureters from adult mice injected with bromophenol blue. Ureters from hydronephrotic *EphA4*$^{gf/gf}$ mice were dilated and displayed a tortuous appearance (*D*) suggesting a defective peristalsis. In contrast, ureters from wild types (*B*) and *EphA4*$^{gf/gf}$ mice without hydronephrosis (*C*) displayed a straight shape. Scale bar = 1 mm.

retrospective study evaluated the proportion of children with ureteropelvic junction obstruction who were diagnosed with hypertension preoperatively and how blood pressure changed after relief of the obstruction (14). de Waard and colleagues (14) found that ~5% of children with ureteropelvic junction obstruction had hypertension, which was normalized following surgery in >90% of all cases. Consequently, the study provides more evidence of hypertension due to hydronephrosis but raises questions about the actual incidence. Since hypertension is rare in children, further studies on older patients are needed.

In neonatal rats and mice, embedding the ureter into the underlying psoas muscle induces partial unilateral ureteral obstruction. With the use of this model for experimental hydronephrosis, a clear relationship has been demonstrated between hydronephrosis and development of hypertension (8, 9). However, since the hydronephrosis was induced 3 wk postpartum when nephrogenesis is considered completed, some degree of uncertainty remains whether the model reflects the clinical disorder. In the present study, we therefore investigated mice with congenital hydronephrosis. Two models were studied; *EphA4*$^{gf/gf}$ mice, which have a high incidence of hydronephrosis due to disturbed embryonic development, as well as standard C57BL/6 mice, where spontaneous hydronephrosis occasionally develops. Interestingly, both groups of hydronephrotic mice displayed hypertension that was salt sensitive, and the blood pressure level correlated with the degree of hydronephrosis. In contrast, *EphA4*$^{+/+}$ mice did not significantly increase their blood pressure during high-salt treatment (+2 mmHg, $P = 0.12$). Consequently, a link between hydronephrosis and development of hypertension has been demonstrated in two different species and in both experimental and congenital models. Considering this fact, in combination with the retrospective study and several case reports, it seems plausible that a relationship also may exist in humans.

Table 1. *Histology of the kidneys from EphA4*$^{+/+}$ *and EphA4*$^{gf/gf}$

	EphA4$^{+/+}$	*EphA4*$^{gf/gf}$	
	Left or right kidney	Most affected kidney	Least affected kidney
KW, mg	127 ± 8	141 ± 11	139 ± 11
KW/BW, ×10^3	5.2 ± 0.2	4.9 ± 0.2	4.8 ± 0.2
HNR	0.03 ± 0.00	0.40 ± 0.06*	0.10 ± 0.01*
Fibrosis	0.4 ± 0.2	1.5 ± 0.2*	1.5 ± 0.2*
Inflammation	0.3 ± 0.3	1.5 ± 0.3*	0.5 ± 0.2†
Tubular changes	0.0 ± 0.0	0.5 ± 0.2*	0.4 ± 0.2
Glomerular changes	0.0 ± 0.0	1.0 ± 0.2*	0.5 ± 0.2
n	8	10	

Values are presented as means ± SE; *n* = number of mice. BW, body weight; KW, kidney weight; HNR, hydronephrotic ratio. *$P < 0.05$, compared with *EphA4*$^{+/+}$. †$P < 0.05$, compared with most affected kidney of *EphA4*$^{gf/gf}$.

Measurements of hydronephrotic ratios showed that all *EphA4*$^{gf/gf}$ mice displayed some degree of pelvic dilation compared with the littermate controls (*EphA4*$^{+/+}$). In general, *EphA4*$^{gf/gf}$ mice displayed unilateral hydronephrosis; however, bilateral pelvic dilatations were observed in some individuals. We cannot exclude the possibility that the *EphA4-EGFP* mutation per se may influence blood pressure, but considering the clear correlation between the hydronephrotic degree and the blood pressure elevation, this assumption seems unlikely. Moreover, in *EphA4*$^{gf/gf}$ mice with the smallest degree of hydronephrosis, the blood pressure was similar to that in the controls. Like humans, mice do also display congenital hydronephrosis and over the past years we have been able to locate a few wild-type mice (C57BL/6J) with spontaneous hydronephrosis that also had salt-sensitive hypertension. Taken together, we do not find it likely that hypertension in *EphA4*$^{gf/gf}$ mice is directly caused by their genotype but rather linked to their hydronephrosis.

Ureteral obstruction is associated with tubular atrophy, interstitial inflammation, and the subsequent loss of nephrons (12). Several experimental models have been established to investigate obstructive nephropathy, of which the most commonly used is complete unilateral ureteral obstruction for a

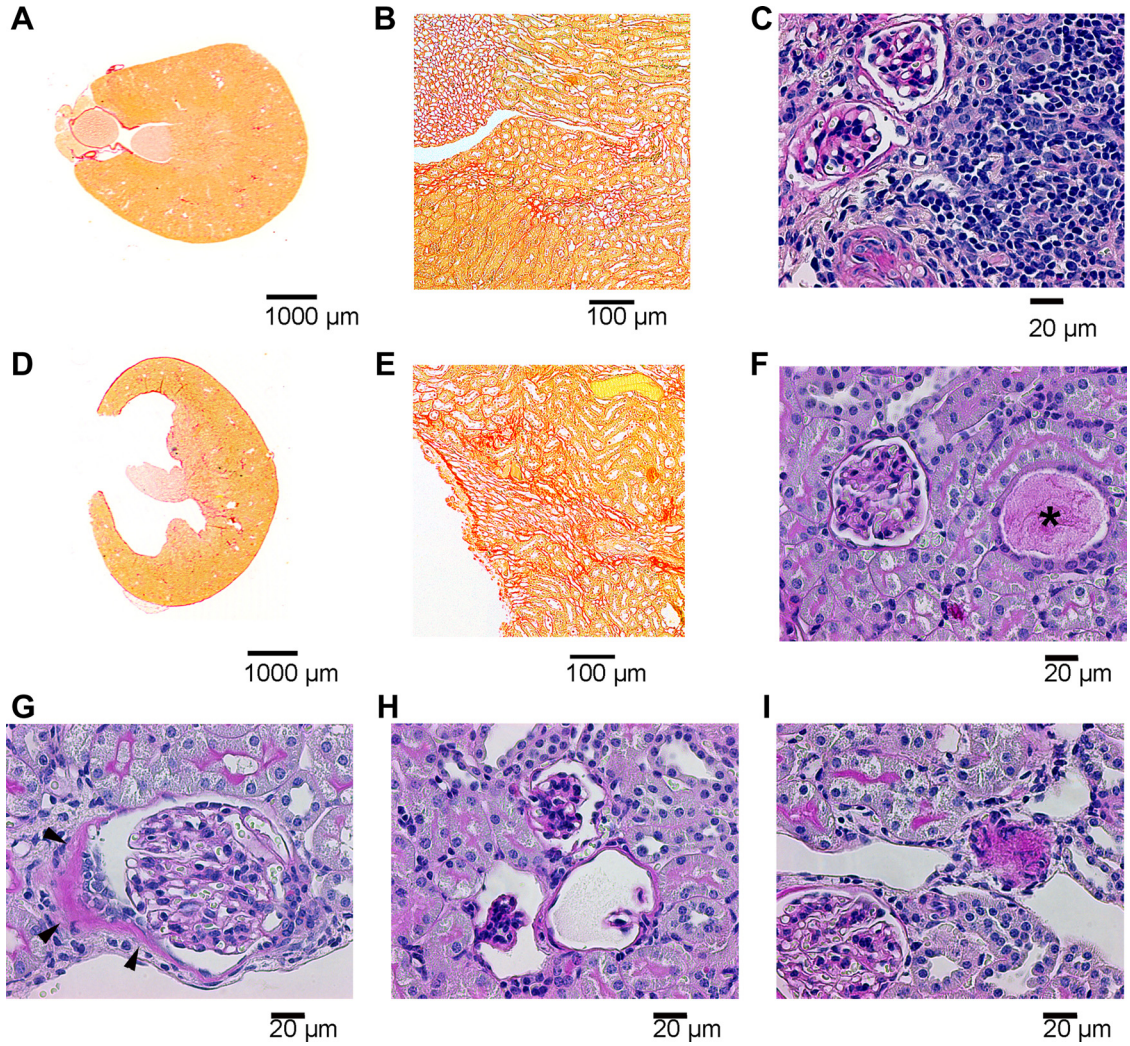

Fig. 8. Representative picro-sirius-stained sections from *EphA4*$^{+/+}$ (*A* and *B*) and *EphA4*$^{gf/gf}$ (*D* and *E*) kidneys. Kidneys of *EphA4*$^{+/+}$ mice have a normal appearance with only minor fibrotic changes, while the *EphA4*$^{gf/gf}$ mice shows pelvic dilatation and areas with pronounced interstitial fibrosis. *C*, *F*, *G*, *H*, and *I*: periodic acid Schiff-stained slides from *EphA4*$^{gf/gf}$ mice. *C*: interstitium showing infiltration of inflammatory cells, predominantly mononuclear cells, disrupting the normal tubular architecture. *F*: dilated tubule with cast (*). Note the shortened height of tubular epithelial cells. Glomerulus seen in this field is normal. *G*: Enlarged glomerulus showing mild pericapsular fibrosis at urinary pole (arrow head). *H*: 3 glomeruli, 1 of them showing collapse of capillary loops. Surrounding tubulointerstitial area is normal. *I*: micrograph showing 1 normal and 1 sclerotic glomeruli surrounded by normal tubules.

short period of time. This type of obstruction is very rare in clinical practice, even though it is often referred to in clinical discussions. The renal outcome following chronic partial ureteral obstruction, which is a far more common disorder, is more relevant from a clinical point of view. In the present study, *EphA4*$^{gf/gf}$ mice with congenital hydronephrosis displayed many of the characteristic features associated with long-term ureteral obstruction and could therefore provide useful information in the future.

The hydronephrotic *EphA4*$^{gf/gf}$ mice displayed reduced renal plasma flow and lower GFR, which most likely is caused by impaired function of the diseased kidney due to altered renal autoregulation and damages to the cortical-medullary region. In earlier studies, hydronephrotic kidneys had increased oxidative stress (6, 18), reduced nitric oxide bioavailability, and a sensitized tubuloglomerular feedback response (5, 7). These changes may protect the hydronephrotic kidney from excessive pressure by reducing glomerular perfusion and filtration but might also play an important role in the development of hypertension by increasing preglomerular resistance and promote fluid and solute retention. In the present study, the GFR values reflect total filtration of both kidneys. Since the nonhydronephrotic kidney in unilateral hydronephrosis, or the least obstructed kidney in bilateral hydronephrosis, increases its function to compensate (23), the actual GFR in the hydronephrotic kidney is probably even lower. In the present study, the histopathological changes found in contralateral kidneys of *EphA4*$^{gf/gf}$ mice with unilateral hydronephrosis are most likely caused by long-term hyperfiltration. However, we cannot fully rule out the possibility that the *EphA4*$^{gf/gf}$ genotype has contributed to the changes.

In the present study, ultrasound was used to visualize the hydronephrotic kidneys. The dilated pelvic area and the reduced blood flow in the kidneys of *EphA4*$^{gf/gf}$ were clearly seen and supports the PAH clearance studies. Consequently, ultrasound appears to be a useful tool for visualization of mouse

kidneys and can be used as a noninvasive method to characterize renal blood flow as well as different degrees of pelvic dilatation.

In earlier studies on rats with experimentally induced PUUO, plasma renin was elevated during normal-sodium conditions but not during low- or high-sodium diets. Furthermore, the plasma renin concentration was not related to the degree of hypertension (9). No differences in renin have been found in mice with experimentally induced PUUO (8). In the present study, plasma renin concentration was not significantly altered in the *EphA4*$^{gf/gf}$ mice compared with wild types. Given that an elevated blood pressure normally suppresses renin, the fact that renin was unaffected in the present study, as well as the earlier mouse model despite hypertension, could indicate a deficient regulation. Consequently, renin might be involved to some extent in the hypertensive development but could not be the sole cause. In further studies, intrarenal renin-angiotensin system components could be characterized since they can be substantially different compared with plasma.

In conclusion, there is a causal link between congenital hydronephrosis and later development of salt-sensitive hypertension and renal damage. Since heart rate was unaltered, increased NaCl intake may increase peripheral resistance and contribute to the observed hypertension in this model. Even though clinical prospective studies are warranted, the present findings together with earlier observations in experimentally induced hydronephrosis strengthen the apprehension that a conservative treatment strategy in hydronephrotic children may lead to hypertension and renal disease later in life.

GRANTS

This study was financially supported by the Swedish Research Council (K2012-99X-21971-01-3, K2009-64X-03522-38-2, K2004-32P-15230, and K2005-33X-15327), Wallenberg Foundation, Wallenberg Consortium North, Swedish Heart and Lung Foundation (20110589 and 20100183), Jeanssons Foundation, Ingabritt and Arne Lundberg Foundation, European Union through European Regional Development Fund, Archimedes Foundation, Fritz Thyssen Foundation, and GARBK6588.

DISCLOSURES

No conflicts of interest, financial or otherwise, are declared by the author(s).

AUTHOR CONTRIBUTIONS

Author contributions: J.S., A.E.G.P., K.K., and M.C. conception and design of research; J.S., C.P., X.G., E.L., A.N., B.L.J., and M.C. performed experiments; J.S., E.L., M.L.O., and M.C. analyzed data; J.S., C.P., E.L., A.N., B.L.J., M.L.O., A.E.G.P., K.K., and M.C. interpreted results of experiments; J.S. and M.C. prepared Figs.; J.S., C.P., E.L., K.K., and M.C. drafted manuscript; J.S., C.P., X.G., A.N., B.L.J., M.L.O., A.E.G.P., K.K., and M.C. edited and revised manuscript; J.S., C.P., X.G., E.L., A.N., B.L.J., M.L.O., A.E.G.P., K.K., and M.C. approved final version of manuscript.

REFERENCES

1. **Amar AD.** Congenital hydronephrosis of lower segment in duplex kidney. *Urology* 7: 480–485, 1976.
2. **Bartram MP, Hohne M, Dafinger C, Volker LA, Albersmeyer M, Heiss J, Gobel H, Bronneke H, Burst V, Liebau MC, Benzing T, Schermer B, Muller RU.** Conditional loss of kidney microRNAs results in congenital anomalies of the kidney and urinary tract (CAKUT). *J Mol Med (Berl)* 2013 Jan 24 [Epub ahead of print].
3. **Bolger PM, Eisner GM, Shea PT, Ramwell PW, Slotkoff LM.** Effects of PGD2 on canine renal function. *Nature* 267: 628–630, 1977.
4. **Carlstrom M.** Causal link between neonatal hydronephrosis and later development of hypertension. *Clin Exp Pharmacol Physiol* 37: e14–23, 2010.
5. **Carlstrom M, Brown RD, Edlund J, Sallstrom J, Larsson E, Teerlink T, Palm F, Wahlin N, Persson AE.** Role of nitric oxide deficiency in the development of hypertension in hydronephrotic animals. *Am J Physiol Renal Physiol* 294: F362–F370, 2008.
6. **Carlstrom M, Brown RD, Sallstrom J, Larsson E, Zilmer M, Zabihi S, Eriksson UJ, Persson AE.** SOD1 deficiency causes salt sensitivity and aggravates hypertension in hydronephrosis. *Am J Physiol Regul Integr Comp Physiol* 297: R82–R92, 2009.
7. **Carlstrom M, Lai EY, Steege A, Sendeski M, Ma Z, Zabihi S, Eriksson UJ, Patzak A, Persson AE.** Nitric oxide deficiency and increased adenosine response of afferent arterioles in hydronephrotic mice with hypertension. *Hypertension* 51: 1386–1392, 2008.
8. **Carlstrom M, Sallstrom J, Skott O, Larsson E, Wahlin N, Persson AE.** Hydronephrosis causes salt-sensitive hypertension and impaired renal concentrating ability in mice. *Acta Physiol (Oxf)* 189: 293–301, 2007.
9. **Carlstrom M, Wahlin N, Sallstrom J, Skott O, Brown R, Persson AE.** Hydronephrosis causes salt-sensitive hypertension in rats. *J Hypertens* 24: 1437–1443, 2006.
10. **Cervenka L, Wang CT, Navar LG.** Effects of acute AT_1 receptor blockade by candesartan on arterial pressure and renal function in rats. *Am J Physiol Renal Physiol* 274: F940–F945, 1998.
11. **Chertin B, Puri P.** Familial vesicoureteral reflux. *J Urol* 169: 1804–1808, 2003.
12. **Chevalier R.** Molecular and cellular pathophysiology of obstructive nephropathy. *Pediatr Nephrol* 13: 612–619, 1999.
13. **Dahmann C, Oates AC, Brand M.** Boundary formation and maintenance in tissue development. *Nat Rev Genet* 12: 43–55, 2011.
14. **de Waard D, Dik P, Lilien MR, Kok ET, de Jong TP.** Hypertension is an indication for surgery in children with ureteropelvic junction obstruction. *J Urol* 179: 1976–1978; discussion 1978–1979, 2008.
15. **Dhillon HK.** Prenatally diagnosed hydronephrosis: the Great Ormond Street experience. *Br J Urol* 81, *Suppl* 2: 39–44, 1998.
16. **Feather SA, Malcolm S, Woolf AS, Wright V, Blaydon D, Reid CJ, Flinter FA, Proesmans W, Devriendt K, Carter J, Warwicker P, Goodship TH, Goodship JA.** Primary, nonsyndromic vesicoureteric reflux and its nephropathy is genetically heterogeneous, with a locus on chromosome 1. *Am J Hum Genet* 66: 1420–1425, 2000.
17. **Grunwald IC, Korte M, Adelmann G, Plueck A, Kullander K, Adams RH, Frotscher M, Bonhoeffer T, Klein R.** Hippocampal plasticity requires postsynaptic ephrinBs. *Nat Neurosci* 7: 33–40, 2004.
18. **Kawada N, Imai E, Karber A, Welch WJ, Wilcox CS.** A mouse model of angiotensin II slow pressor response: role of oxidative stress. *J Am Soc Nephrol* 13: 2860–2868, 2002.
19. **Liapis H.** Biology of congenital obstructive nephropathy. *Nephron Exp Nephrol* 93: e87–91, 2003.
20. **Lifland JH.** Ureteropelvic obstruction of duplex kidney. *Urology* 6: 603–604, 1975.
21. **Livera LN, Brookfield DS, Egginton JA, Hawnaur JM.** Antenatal ultrasonography to detect fetal renal abnormalities: a prospective screening programme. *BMJ* 298: 1421–1423, 1989.
22. **Lykkegard S, Poulsen K.** Ultramicroassay for plasma renin concentration in the rat using the antibody-trapping technique. *Anal Biochem* 75: 250–259, 1976.
23. **Morsing P, Stenberg A, Wahlin N, Persson AE.** Tubuloglomerular feedback in rats with chronic partial bilateral ureteral obstruction. *Renal Physiol Biochem* 18: 27–34, 1995.
24. **Nakai H, Asanuma H, Shishido S, Kitahara S, Yasuda K.** Changing concepts in urological management of the congenital anomalies of kidney and urinary tract, CAKUT. *Pediatr Int* 45: 634–641, 2003.
25. **Nusbacher N, Bryk D.** Hydronephrosis of the lower pole of the duplex kidney: another renal pseudotumor. *AJR Am J Roentgenol* 130: 967–969, 1978.
26. **Ogita H, Kunimoto S, Kamioka Y, Sawa H, Masuda M, Mochizuki N.** EphA4-mediated Rho activation via Vsm-RhoGEF expressed specifically in vascular smooth muscle cells. *Circ Res* 93: 23–31, 2003.
27. **Pasquale EB.** Eph-ephrin bidirectional signaling in physiology and disease. *Cell* 133: 38–52, 2008.

28. **Pitulescu ME, Adams RH.** Eph/ephrin molecules–a hub for signaling and endocytosis. *Genes Dev* 24: 2480–2492, 2010.
29. **Podevin G, Mandelbrot L, Vuillard E, Oury JF, Aigrain Y.** Outcome of urological abnormalities prenatally diagnosed by ultrasound. *Fetal Diagn Ther* 11: 181–190, 1996.
30. **Sallstrom J, Friden M.** Simultaneous determination of renal plasma flow and glomerular filtration rate in conscious mice using dual bolus injection. *J Pharmacol Toxicol Methods* 67: 187–193, 2013.
31. **Schlussel R, Retik A.** Ectopic ureter, ureterocele, and other anomalies of the ureter. In: *Campbell-Walsh Urology*, edited by Wein A. Philadelphia, PA: Saunders, 2007, p. 3393–3413.
32. **Sekine T, Miyazaki H, Endou H.** Molecular physiology of renal organic anion transporters. *Am J Physiol Renal Physiol* 290: F251–F261, 2006.
33. **Thomas DF.** Fetal uropathy. *Br J Urol* 66: 225–231, 1990.
34. **Ulman I, Jayanthi VR, Koff SA.** The long-term followup of newborns with severe unilateral hydronephrosis initially treated nonoperatively. *J Urol* 164: 1101–1105, 2000.
35. **Wiesel A, Queisser-Luft A, Clementi M, Bianca S, Stoll C.** Prenatal detection of congenital renal malformations by fetal ultrasonographic examination: an analysis of 709,030 births in 12 European countries. *Eur J Med Genet* 48: 131–144, 2005.